Eur Radiol (2003) 13:672–685
DOI 10.1007/s00330-002-1477-0

A. Bueno Horcajadas
J. López Lafuente
R. de la Cruz Burgos
S. Hernández Muñiz
S. Alonso Roca
S. González Ortega
P. Dominguez Franjo
E. Ortiz Cruz

Ultrasound and MR findings in tumor and tumor-like lesions of the fingers

Received: 23 August 2001
Revised: 26 February 2002
Accepted: 21 March 2002
Published online: 15 June 2002

This work was originally presented in the framework of the scientific exhibition at ECR 2001 entitled: "Magnetic resonance and sonography of the finger anatomy and in the diagnosis of finger pathology".

A.B. Horcajadas (✉) · J.L. Lafuente
R. de la Cruz Burgos · S.H. Muñiz
S.A. Roca · S.G. Ortega · E.O. Cruz
Department of Radiology,
Fundación Hospital de Alcorcón,
C/ Budapest, 1, 28922 Alcorcón,
Madrid, Spain
e-mail: AbuenoHorcajadas@fhalcorcon.es
Tel.: +34-91-6219574
Fax: +34-91-6219901

P.D. Franjo
Department of Pathology,
Fundación Hospital de Alcorcón,
C/ Budapest, 1, 28922 Alcorcón,
Madrid, Spain

E.O. Cruz
Department of Orthopedics,
Fundación Hospital de Alcorcón,
C/ Budapest, 1, 28922 Alcorcón,
Madrid, Spain

Abstract Finger lesions are a frequent problem because of their functional significance and their small size. Because of this, the radiologist has an important role to play in the correct presurgical diagnosis. The aim of this article is to describe the anatomy and the characteristic US and MR findings of the most common tumor and tumor-like lesions of the fingers, and to discuss the differential diagnosis in cases of unspecific or non-diagnostic findings. We present representative cases selected from 62 patients evaluated at our institution, with pathologic correlation.

Keywords Finger · Anatomy · Tumor · Magnetic resonance · Ultrasound

Introduction

Surgeons need to know both the exact location of the finger lesions in relation to the anatomic structures and the correct presurgical diagnosis. This is why it is important to possess an in-depth knowledge of radiological finger anatomy and also to acquire a profound knowledge of the radiological appearance of the different pathologic entities. Imaging tissue characterization is also important because it is easier to achieve a correct diagnosis if it is known from which tissue a lesion originates. Both US and MR are useful techniques; however, the literature on US and MR on finger anatomy and pathology was scarce until recently [1, 2, 3, 4, 5, 6, 7].

In this article we do not attempt to debate on all possible finger pathologies. We describe the finger anatomic details and we depict the imaging findings of the most common tumors and tumor-like lesions of the fingers, with two complementary imaging techniques: US and MR. Ultrasound is an inexpensive and accessible technique but is operator dependent. Magnetic resonance is less widely available but obtains a very good tissue contrast and it can evaluate bone.

Patients and methods

We retrospectively reviewed the US and MR examinations, clinical histories, and radiographs in 62 consecutive patients (37 women and

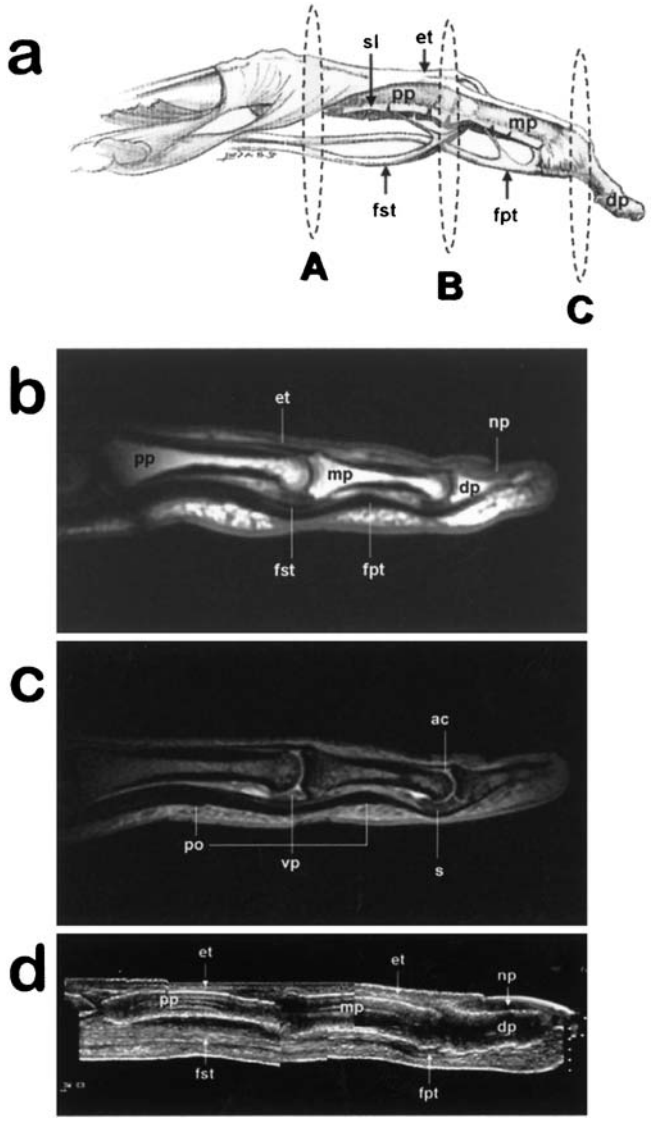

Fig. 1a–d Sagittal anatomic images. **a** Sagittal image of finger. **b** Sagittal T1-weighted spin-echo (SE) MR image (TR/TE/slice thickness: 400 ms/14 ms/2 mm). **c** Sagittal gradient-echo (GE) MR image (TR/TE/slice thickness: 400 ms/14 ms/2 mm, flip angle 20°). **d** Sagittal ultrasound image. *ac* articular cartilage; *dp* Distal phalanx; *et* extensor expansion tendon; *fst* flexor digitorum superficialis tendon; *fpt* flexor digitorum profundus tendon; *mp* middle phalanx; *np* nail plate; *po* pulley of the flexor tendon; *pp* proximal phalanx; *s* sesamoid bone; *sl* sheath laid; *vp* volar plate

25 men; mean age 47 years, SD 19 years) who attended our institution during the previous 2 years with clinical tumors in the fingers.

The MR was performed in all 62 patients on a GE Signa Horizon LX 1.5-T system (General Electric, Milwaukee, Wis.). Superficial and anteroposterior gradient coils were used. Several sequences were acquired: spin-echo (SE) T1-weighted (TR 400–620 ms/TE 12–20 ms) and fast spin-echo (FSE) DP and T2-weighted (TR 3000–6000 ms/TE 18–120 ms/echo train length 8) with and without fat suppression; gradient-echo (TR 400 ms/TE 14 ms/flip angle 20°), and short time inversion recovery (STIR; TR 3400–3700 ms/TE 36–43 ms/TI 150 ms). A 256×160–256 acquisition matrix with a field of view according to the lesion size was used (8–16 cm). Forty-three patients received an IV injection of Gd-DTPA. The Gd-DTPA was not used in those cases where it would not have contributed to the characterization of the lesion, such as typical tenosynovitis, joint synovitis or lipoma. Twenty-eight patients were also studied on a GE Logic 700 US with a multifrequency probe (7–13 MHz), and they were studied with echo Doppler. Longitudinal consecutive sagittal planes and axial planes were obtained, both from dorsal and palmar sides, in the sonographic anatomic evaluation. Afterwards, a single image was created using graphics software (Microsoft Photo Editor 3.0, Paint Shop Pro 6.01). The US and MR images were stored using a picture archiving and communications system (PACS) GE system (12.2.i) with DICOM (3.0) format. Selected images were converted to TIIF format using GE Radworks Diagnostic (5.0) program. The US and MR images were retrospectively evaluated, taking into account the plain X-ray film findings and the clinical history. Surgery and pathologic correlation were performed in 37 patients. The US and MR anatomic details were correlated with our original reference diagram. We describe and discuss the characteristic US and MR findings of the selected cases of tumor and tumor-like lesions of the fingers with pathologic correlation.

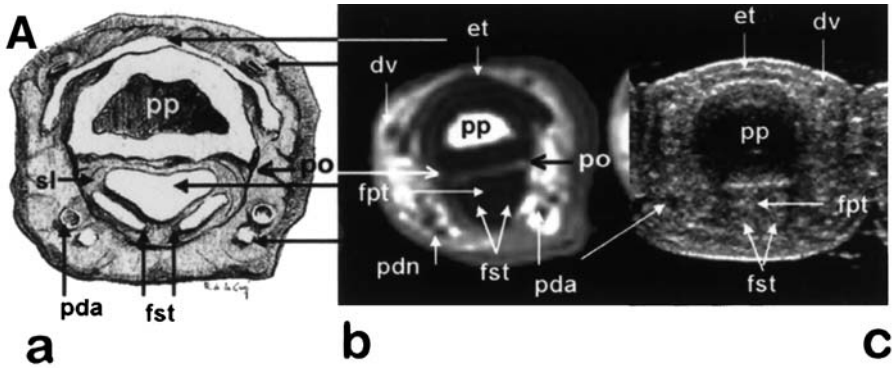

Fig. 2a–c Axial anatomic images at the levels A, B, and C of Fig. 1a (proximal, middle, and distal phalanges, respectively). *Ac* Articular cartilage; *cl* collateral ligament; *ddv* digital dorsal vein; *dp* distal phalanx; *et* extensor expansion tendon; *fst* flexor digitorum superficialis tendon; *fpt* flexor digitorum profundus tendon; *mp* middle phalanx; *np* nail plate; *pda* palmar digital artery; *pdn* palmar digital nerve; *pp* proximal phalanx; *po* pulley of the flexor tendon; *sl* sheath laid; *vp* volar plate. **a** Axial picture. **b** Axial T1-weighted SE MR image (TR/TE/slice thickness: 480 ms/14 ms/4 mm). **c** Axial ultrasound image

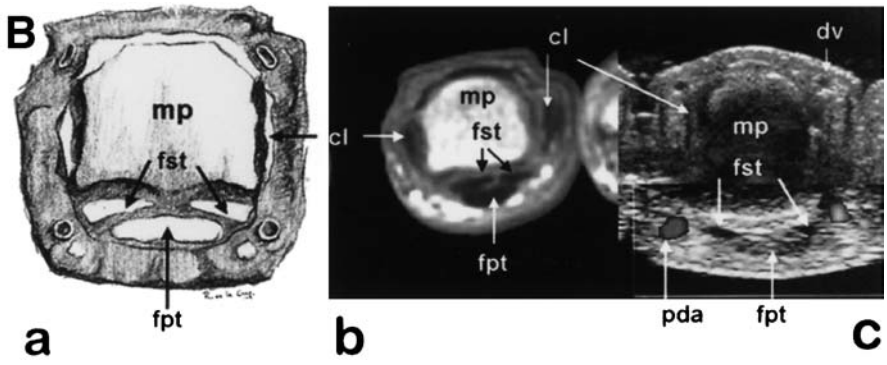

Fig. 3a–c Axial anatomic image at the levels A, B, and C of Fig. 1a (proximal, middle, and distal phalanges respectively). **a** Axial image. **b** Axial T1-weighted SE MR image (TR/TE/slice thickness: 480 ms/14 ms/4 mm). **c** Axial ultrasound image

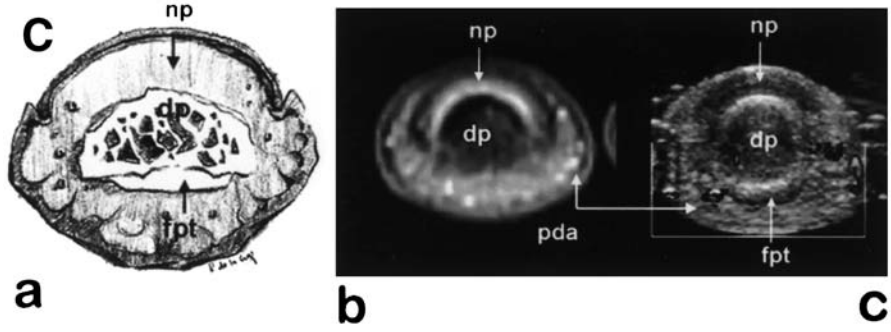

Fig. 4a–c Axial anatomic images at the levels A, B, and C of Fig. 1a (proximal, middle, and distal phalanges, respectively). **a** Axial image. **b** Fast spin-echo proton-density (FSE PD) fat-suppressed MR image (TR/TE/slice thickness: 3000 ms/43 ms/4 mm). **c** Axial ultrasound image

Anatomy

The basic anatomic elements of the fingers are the phalanges and their articulations, a tendinous extensor mechanism, a tendinous flexor mechanism, the vessels, and the nerves. The number of extensor tendons of the fingers is variable, mainly distal to the extensor retinaculum, and they are not organized in digitorum superficialis and profundus tendons as are the flexor tendons. The metacarpophalangeal joint capsule and the lumbrical and interosseous tendons contribute to the extensor mechanism, because they form the dorsal interosseous ligament, which laterally reinforces the extensor tendon (Fig. 1a) [8]. The flexor mechanism consists of two tendons in each finger: the flexor digitorum superficialis tendon and the flexor digitorum profundus tendon. The former inserts into the middle phalanx, but first it splits into two halves, opposite the proximal phalanx, leaving a slit through which the flexor digitorum profundus tendon passes, which attaches distally on the distal phalanx. This anatomic circumstance results in a characteristic morphology and disposition of the flexor tendons on axial scans, which varies depending on the level of the section (Figs. 2, 3, 4); and care must be taken not to mistake normal findings for a tendinous lesion.

The echogenicity of the tendon differs depending on the incidence angle of the ultrasound beam, due to the inosotropic quality of the tendon. When the incidence is perpendicular to the tendons, the echogenicity is the highest and shows a characteristic fibrillar echo structure, whereas the tendon appears more hypoechogenic,

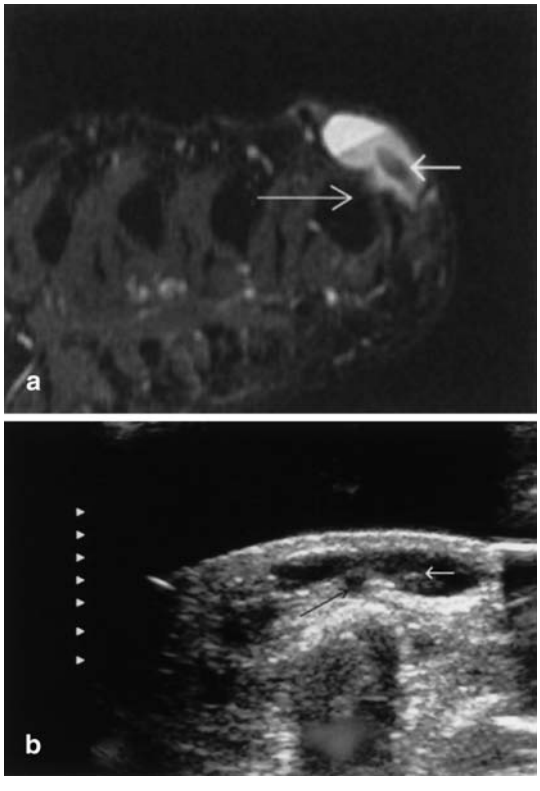

Fig. 5a, b Synovial cyst. **a** Axial short time inversion recovery (STIR; TR/TE/slice thickness: 3640 ms/36 ms/3 mm, 140 ms inversion time) MR image. **b** Ultrasound image. Lobulated well-circunscribed hyperintense and anechogenic lesion arising from the joint. The stalk (*long arrow*) of the cyst and the fibrous component (*short arrow*) are conspicuous

Fig. 6 Synovial cyst. Sagittal contrast-enhanced T1-weighted SE image (TR/TE/slice thickness: 500 ms/12 ms/3 mm). The synovial lining enhances after intravenous gadolinium (Gd) administration (*arrow*)

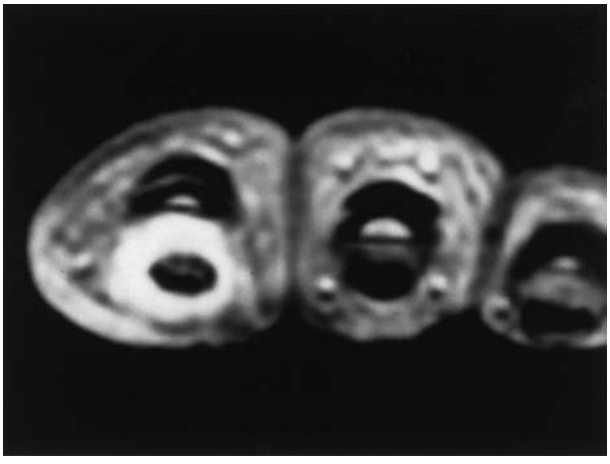

Fig. 7 Typical tenosynovitis. Axial T2-weighted GE image (TR/TE/slice thickness: 400 ms/14 ms/3 mm, flip angle 20°). Flexor tendons surrounded by fluid inside a homogeneous tendon sheath

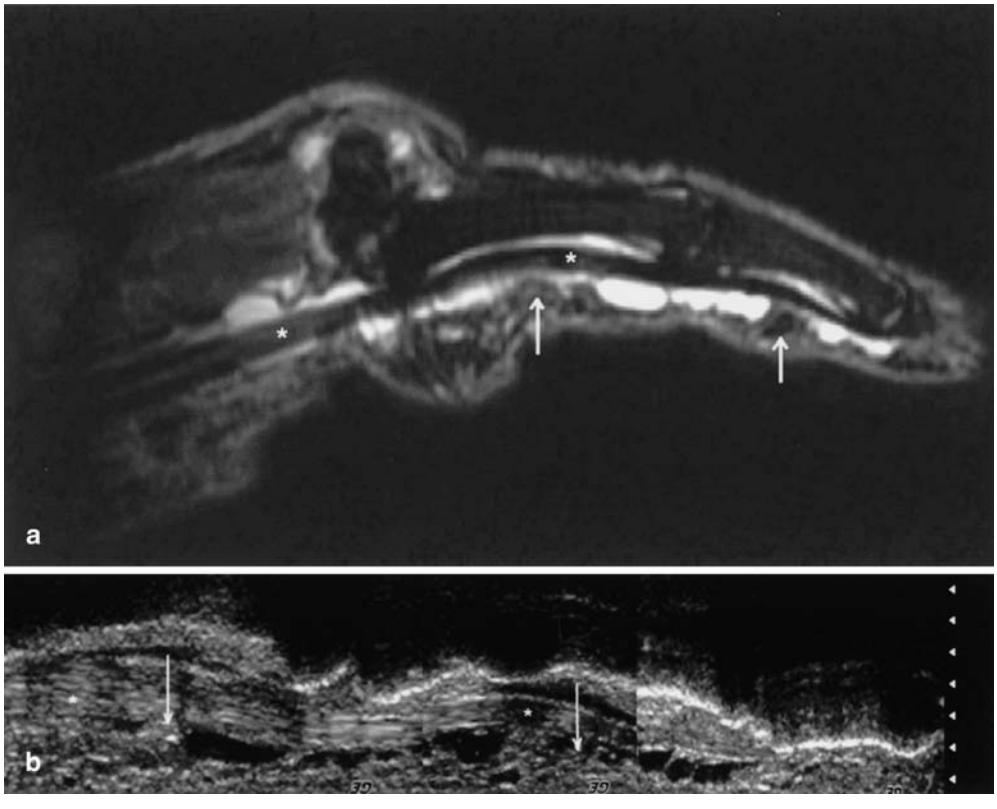

Fig. 8a, b Chronic tenosynovitis. **a** Sagittal STIR image (TR/TE/slice thickness: 3420 ms/43 ms/4 mm, 150 ms inversion time). **b** Ultrasound image. Fluid (hyperintense on STIR image and anechogenic on US image) within the tendon sheath and thickening of the synovium (*arrows*). There are no tendinous abnormalities. *Asterisk* indicates normal tendon

as the incidence is less perpendicular (Figs. 1d, 2c, 3c, 4c) [1, 9, 10]. This circumstance must not be mistaken for a tendinous lesion. A real lesion must always be demonstrated in two perpendicular planes, which is why the combination of longitudinal and transverse scans is mandatory.

The sheath of the flexor tendons is reinforced by fibrous bands that attach to the periosteum at different places of the phalanx, which are known as pulleys (Figs. 1c, 2) [11, 12]. The interphalangeal articular capsule has another reinforcement, the volar plate (Fig. 1c) [13].

The different structures of the neurovascular bundle run longitudinally along the angles of the finger, and they are readily identified on an axial plane. The main neurovascular structures at the dorsal angles are the dorsal digital veins, and at the volar angles are the palmar digital artery and the digital nerve (Figs. 2, 3, 4). The displacement of these vessels may be the key to discovering the original tissue of a tumor. For example, a giant cell tumor of the tendon sheath typically displaces the vessels excentrically. The final anatomic structure is the nail bed (Figs. 1, 4), which is located dorsal to the distal phalanx. Some specific lesions characteristically arise from this structure [14].

Synovial and ganglion cyst

A synovial cyst is a herniation of the synovial membrane through the joint capsule. In contrast, the ganglion cyst rarely communicates with the synovium of a tendon sheath or joint, and it is not lined by synovium. They are usually attached to the tendon sheath of the hands and feet [4, 15]. In our experience they are frequently small lesions (a few millimeters), which may present themselves clinically as hard small nodes. Characteristic MR findings include a well-circumscribed homogeneous lesion, highly hyperintense on T2-weighted spin-echo (SE) and on short time inversion recovery (STIR) MR sequences (Fig. 5a), with enhancement of a thin wall after IV gadolinium (Fig. 6). The synovial cysts often show a pedicle to an adjacent joint or tendon sheath (Fig. 5) [16]. On T1-weighted MR images the signal intensity ranges from hypo- to isointense signal, depending on its protein content. They may present fibrous content, hypointense on T2-weighted MR images (Fig. 5). Sometimes there are sharply defined internal septa. They can be associated with trauma, degenerative joint disease, or inflammatory processes [15, 16]. Sonographically, they are typically cystic lesions (Fig. 5b) which may present floating echoes or internal septa. They do not show vascular flow in Doppler examination [1, 4, 17].

The diagnosis is usually straightforward in typical cases with the above-mentioned characteristic findings. The differential diagnosis may include epidermal inclusion cysts and, when the cysts are irregular or ruptured, degenerative and inflammatory lesions [16].

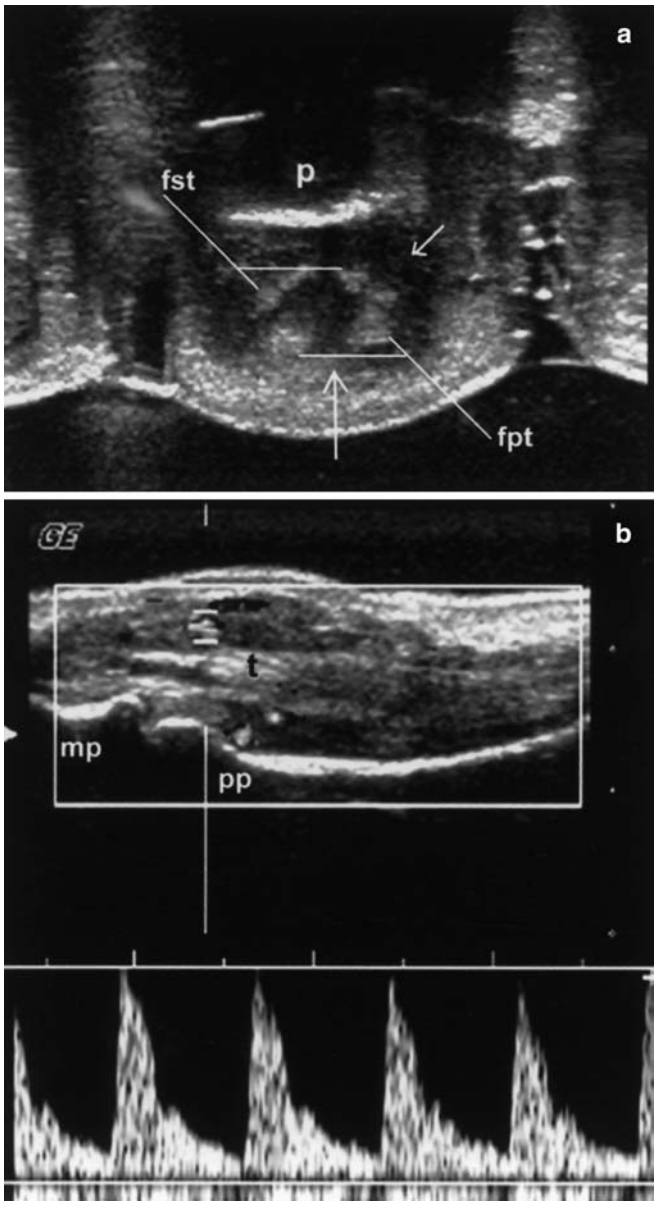

Fig. 9a, b Rheumatoid arthritis with hypertrophic tenosynovitis. **a** Axial ultrasound image. **b** Sagittal duplex Doppler image. Flexor tendon surrounded by hypertrophic synovial seen as a soft tissue (*arrow*), and fluid (*small arrow*). The hypertrophic synovium presents evident arterial Doppler flow. *mp* middle phalanx; *p* phalanx; *pp* proximal phalanx; *t* flexor tendon

Tenosynovitis

Tenosynovitis is the presence of fluid surrounding the tendon, inside its tendon sheath. In the typical tenosynovitis the fluid is depicted within the homogeneous tendon sheath with high signal on T2-weighted and STIR images as the characteristic MR finding (Fig. 7) [2, 3]. The tendon is well observed on US surrounded by an-

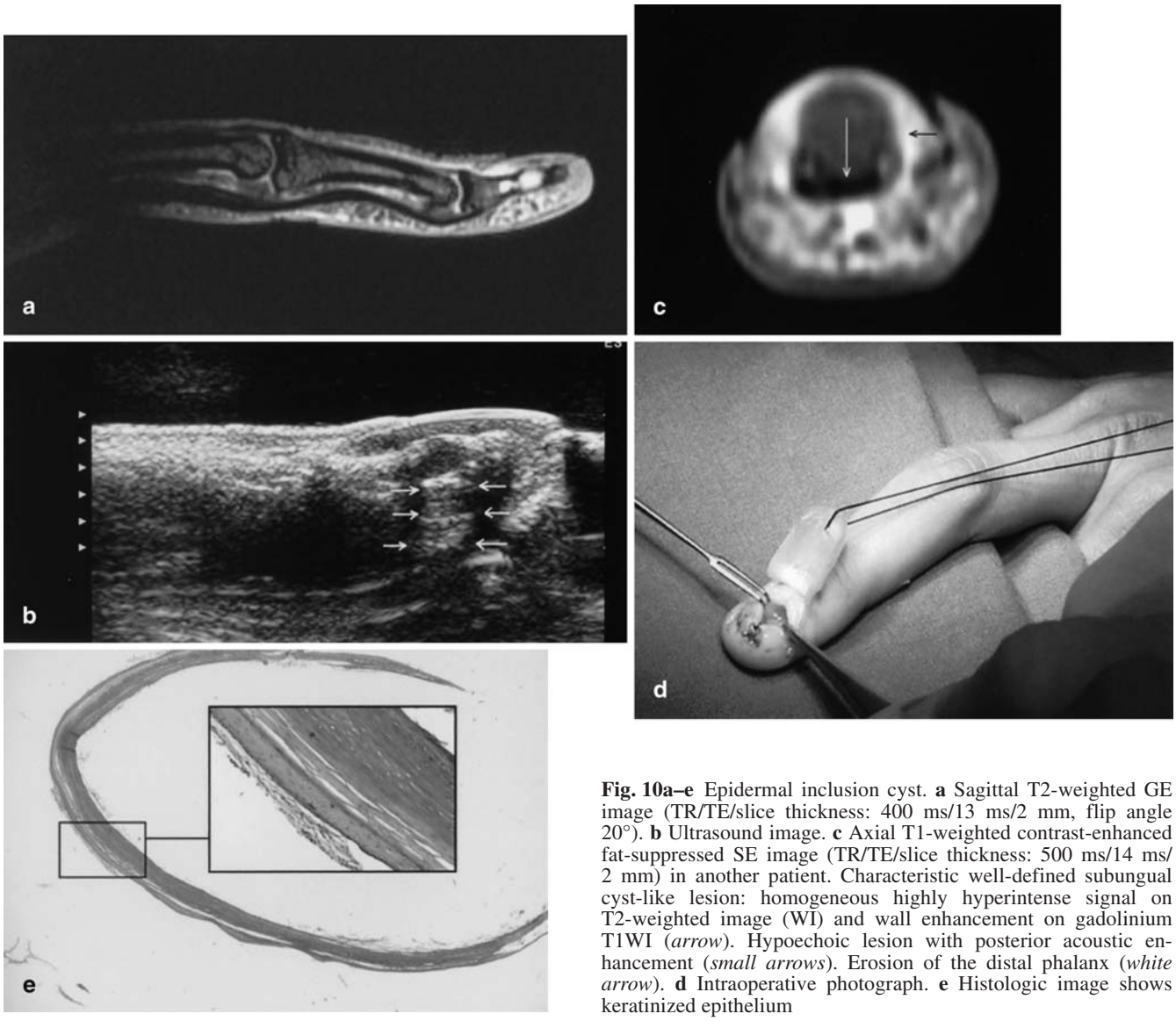

Fig. 10a–e Epidermal inclusion cyst. **a** Sagittal T2-weighted GE image (TR/TE/slice thickness: 400 ms/13 ms/2 mm, flip angle 20°). **b** Ultrasound image. **c** Axial T1-weighted contrast-enhanced fat-suppressed SE image (TR/TE/slice thickness: 500 ms/14 ms/2 mm) in another patient. Characteristic well-defined subungual cyst-like lesion: homogeneous highly hyperintense signal on T2-weighted image (WI) and wall enhancement on gadolinium T1WI (*arrow*). Hypoechoic lesion with posterior acoustic enhancement (*small arrows*). Erosion of the distal phalanx (*white arrow*). **d** Intraoperative photograph. **e** Histologic image shows keratinized epithelium

echogenic fluid. Alterations in the characteristic fibrillar tendon echo structure and girth, or in the MR morphology and signal intensity, may be found, due to tendinitis or tendinosis [1, 4, 10, 17]. Atypical hypertrophic tenosynovitis (Fig. 8) is associated with synovial thickening. It occurs in inflammatory disorders (such as rheumatoid and psoriatic arthritis), crystal-induced arthritis, granulomatous amyloid deposits, or following trauma [6, 18, 19]. Contrast-enhanced Gd-DTPA MR has proved very useful in the evaluation of inflammatory arthritis [19], but echo-Doppler ultrasonography is also very useful in the evaluation of inflammatory tenosynovitis both in the acute phase, in which it can distinguish the inflamed synovial from the synovial fluid by using power/color Doppler US (Fig. 9), as well as in the follow-up of these lesions [20]. Sometimes the synovial thickening may be so great with such a great deal of proliferation that it may have a tumor-like appearance. In this case, the differential diagnosis may include nodular tenosynovitis or giant cell tumor of the tendon sheath and fibroma of the tendon sheath.

Epidermal inclusion cyst

An epidermal inclusion cyst is a smooth round nodule usually in a subungual location, in a patient who has a history of previous trauma. It is a cyst-like lesion: it appears iso-/hypointense on T1-weighted MR images and hyperintense on T2-weighted MR images, with wall enhancement after gadolinium administration [21]; and it is anechoic or hypoechoic with lateral shadows and

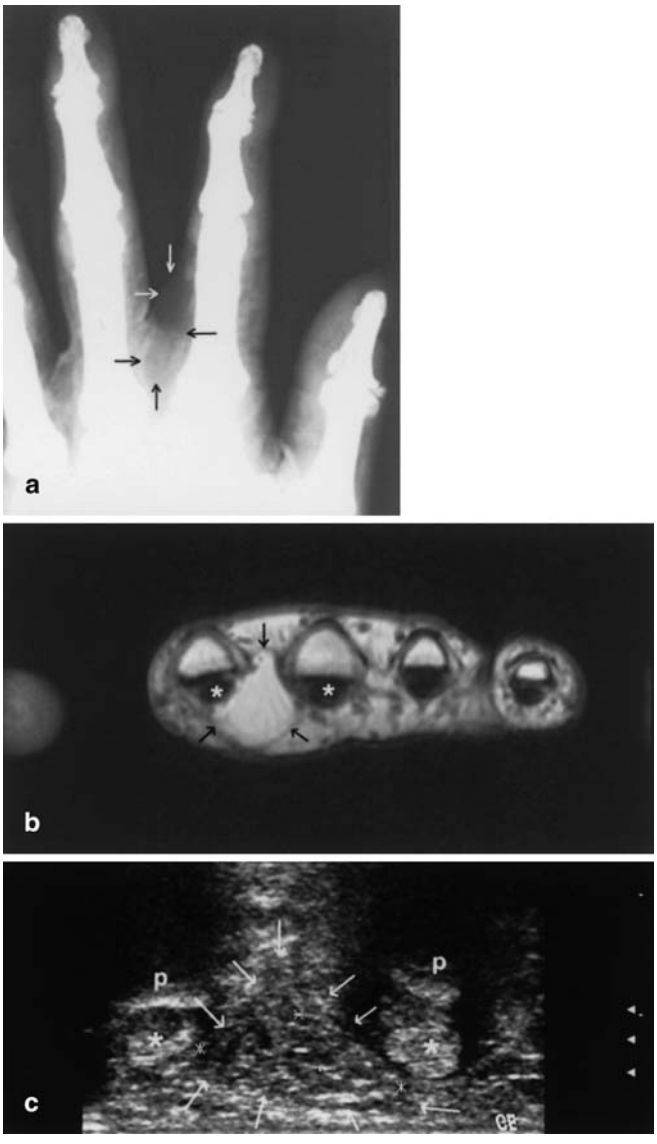

Fig. 11a–c Lipoma. **a** Low-kilovoltage plain radiograph. **b** Axial T1-weighted SE image (TR/TE/slice thickness: 420 ms/15 ms/ 4 mm). **c** Axial ultrasound image. Homogeneous well-delineated mass (*arrows*) between the flexor tendons (*asterisks*) of second to third fingers isointense and slightly hypoechogenic to subcutaneous fat. *p* phalanx

posterior acoustic enhancement on US (Fig. 10). A characteristic feature of this lesion is that it may produce scalloping or a radiolucent lesion in the distal phalanx which underlies the nail bed, so it may be difficult on plain films to differentiate from osseous lesions, such as enchondroma or giant cell tumor, and from glomic tumor [14, 22]. Luckily, neither of these processes behave as a cyst-like lesion after gadolinium administration.

Lipoma

Lipoma is the most common mesenchymal tumor. In the finger it is usually a subcutaneous benign tumor. Its characteristic imaging features are those of a homogeneous, well-circumscribed and encapsulated mass of fatty nature (isointense to fat tissue on MR) [2, 3, 22] and slightly hyper- or hypoechogenic to the subcutaneous fat on US (Fig. 11) [1, 4, 17].

A variant of lipoma is the lipoma of the tendon sheath, which is a mass in every way similar to a simple lipoma that spreads along the tendon sheath. Lipomatous tumors with irregular borders and inhomogeneous signal intensity and echogenicity are rare in the fingers. These are lesions with a tumoral component of non-fatty nature. The differential diagnosis includes liposarcoma and variants of lipoma such as lipoblastoma (which occurs mostly in children), spindle cell lipoma and pleomorphic lipoma (typically as a neck or shoul-

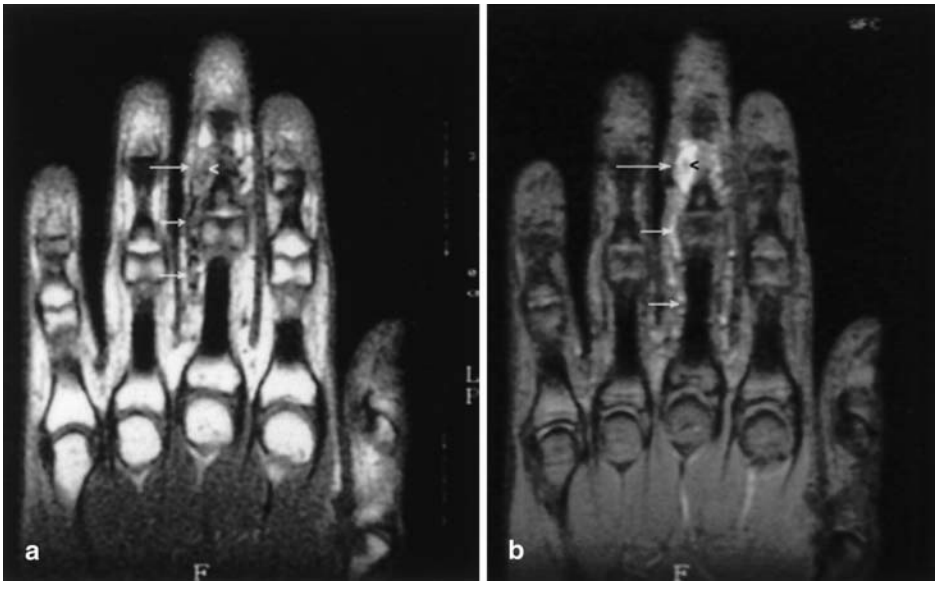

Fig. 12a, b Hemangioma. **a** Coronal contrast-enhanced T1-weighted SE image (TR/TE/ slice thickness: 440 ms/15 ms/ 4 mm). **b** Coronal T2-weighted GE image (TR/TE/slice thickness: 500 ms/14 ms/4 mm, flip angle 20°). Serpiginous tubular tumor (*short arrows*) in the cubital side of the third finger. It is highly hyperintense on T2WI and it shows a hyperintense area on T1WI (*long arrow*) due to blood in dilated channels and fatty elements. Central area of signal void (*arrowhead*) which corresponds to a phlebolith

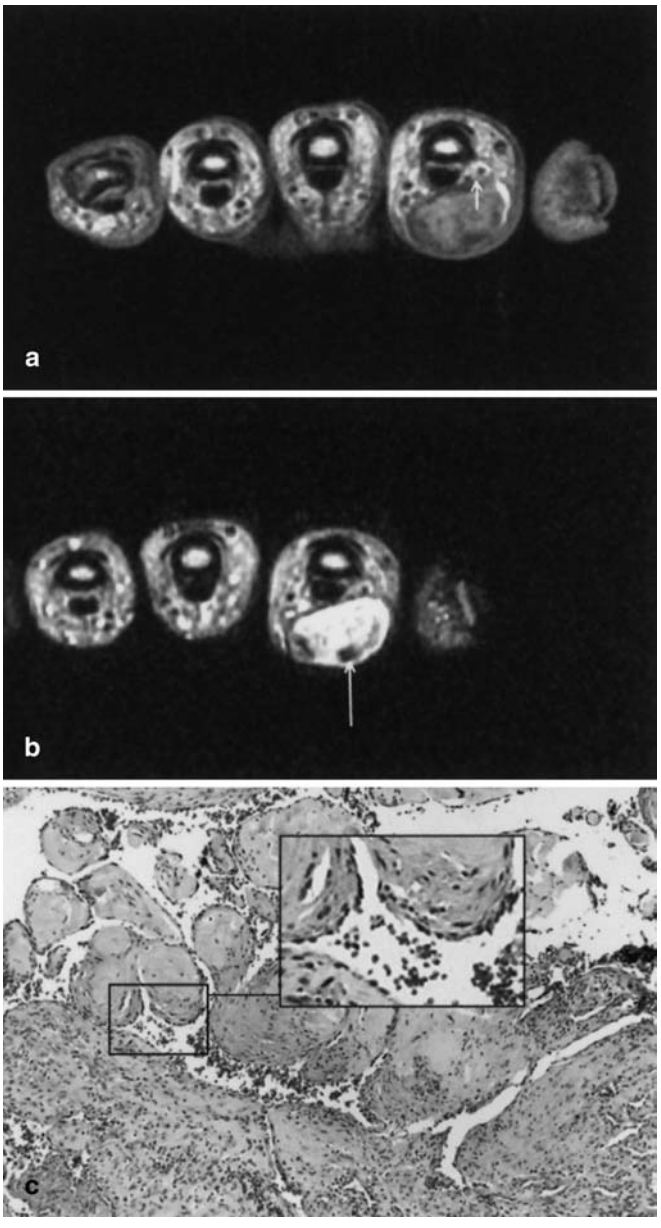

Fig. 13a–c Venous hemangioma with papillary endothelial hyperplasia. **a** Axial contrast-enhanced T1-weighted SE image (TR/TE/slice thickness: 500 ms/15 ms/3 mm). **b** Axial T2-weighted fat-suppressed FSE image (TR/TE/slice thickness: 2560 ms/108 ms/3 mm). Well-defined tumor with a thin capsule. It is hyperintense on T2WI with hypointense foci (*arrow*) and it enhances after IV gadolinium administration. It is superficial to the tendon sheath and it displaces the palmar neurovascular bundle (*small arrow*). **c** Histologic image shows venous elements with areas of papillary endothelial hyperplasia

der subcutaneous mass in men older than 45 years), angiolipoma (particularly in the forearm as an infiltrating mixed mass which is composed of fatty and vascular elements, hyperintense on T1- and T2-weighted MR images with a high enhancement after intravenous contrast), and neural fibrolipoma (which chiefly involves the median nerve in the forearm, wrist or hand, as a tortuous tubular mass within a predominantly fatty mass) [23].

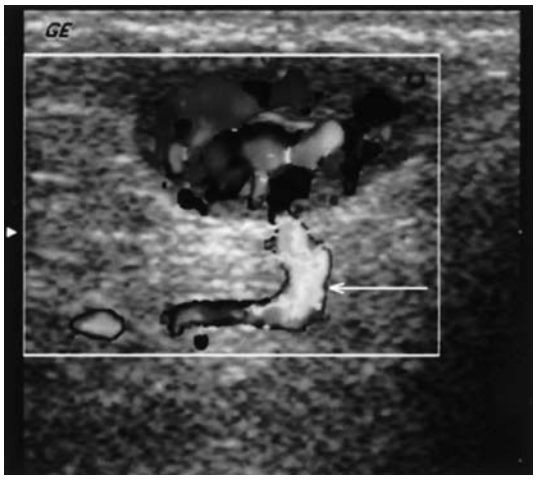

Fig. 14 Angioleiomyoma. Color Doppler image shows a well-defined subcutaneous soft tumor with high Doppler flow. This technique is the modality of choice to differentiate between slow and high flow in these vascular tumors. The afferent vessel is conspicuous (*arrow*)

Hemangioma

Hemangioma is defined as "a benign but non-reactive process in which there is an increase in the number of normal or abnormal-appearing vessels" [24]. Heterogeneous high signal intensity on T2 is the most characteristic MR finding. The radiological appearance may range from a serpiginous tubular pattern with hyperintense strands on T1 (due to blood in dilated channels and fatty elements) and flow void artifacts, which is diagnostic (Fig. 12), to a non-specific appearance [2, 3, 21, 25, 26].

In our series it was not frequently the diagnostic pattern (only 1 case); however, we found a characteristic pattern in 4 of 9 cases: a heterogeneous tumor with high signal on T2 and markedly hypointense foci due to thrombus; and strong enhancement after gadolinium administration (Fig. 13); two of these had areas of papillary endothelial hyperplasia (Masson's angioma; Fig. 13). Variants of benign vascular tumors include intramuscular angiolipoma (which may appear slightly hyperintense on T1-weighted MR images) and angioleiomyoma (2 cases in our series) as a quite homogeneous solid mass, with small tubular structures and high arteriovenous flow on echo Doppler (Fig. 14) [25, 27]. Hemangioma may be difficult to differentiate from post-traumatic hematoma, which usually has low signal intensity on T2-weighted MR image owing to methemoglobin deposits, and peripheral enhancement after gadolinium injection [26]. When the lesion involves the nail bed, differential diagnosis must be done also with a glomus tumor, which usually produces bone erosion [14,

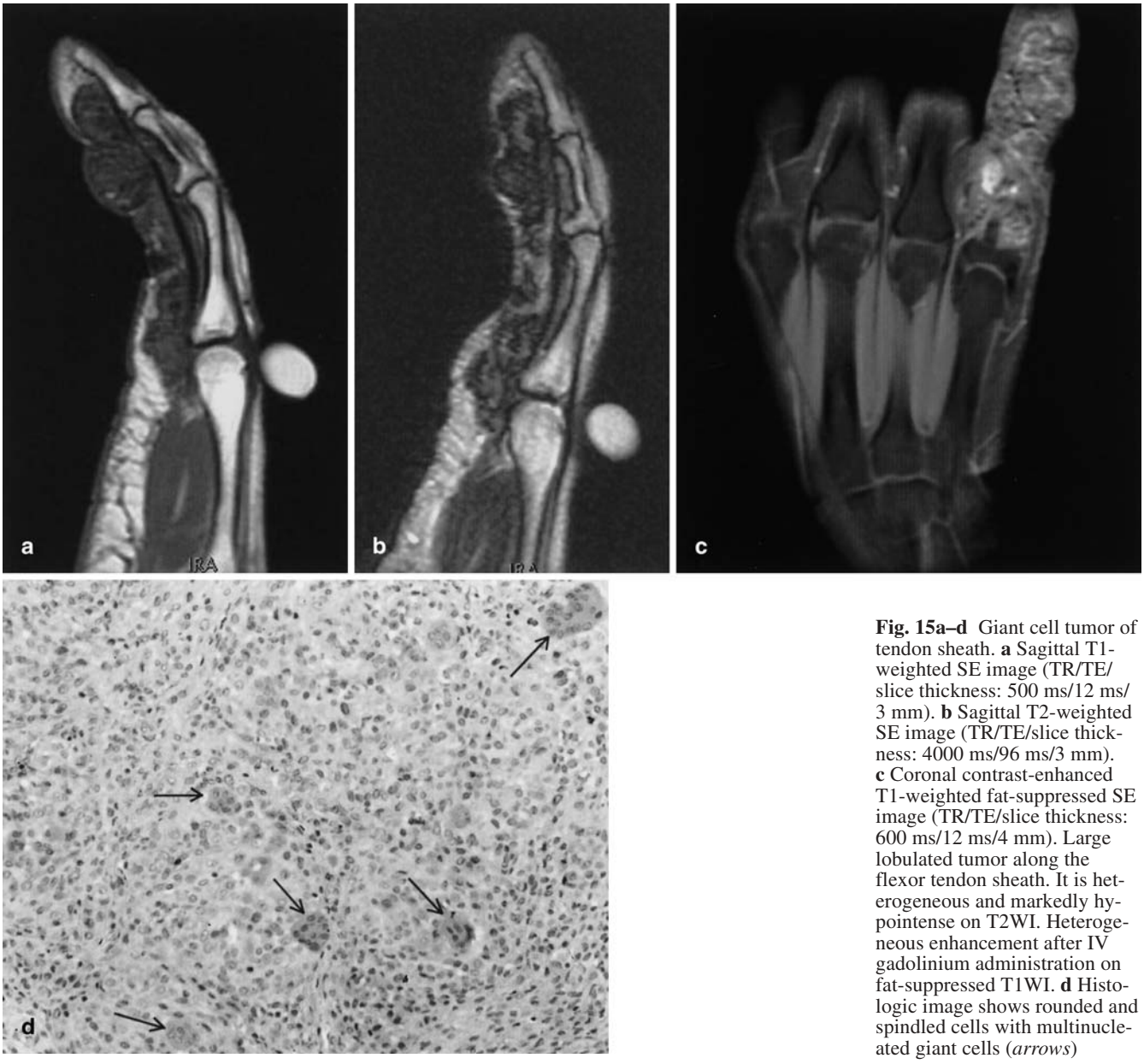

Fig. 15a–d Giant cell tumor of tendon sheath. **a** Sagittal T1-weighted SE image (TR/TE/slice thickness: 500 ms/12 ms/3 mm). **b** Sagittal T2-weighted SE image (TR/TE/slice thickness: 4000 ms/96 ms/3 mm). **c** Coronal contrast-enhanced T1-weighted fat-suppressed SE image (TR/TE/slice thickness: 600 ms/12 ms/4 mm). Large lobulated tumor along the flexor tendon sheath. It is heterogeneous and markedly hypointense on T2WI. Heterogeneous enhancement after IV gadolinium administration on fat-suppressed T1WI. **d** Histologic image shows rounded and spindled cells with multinucleated giant cells (*arrows*)

26]. It is very rare to find malignant vascular tumors in the fingers. The differential diagnosis must be done when there is tumoral necrosis and may include angiosarcoma (most frequently up to 20 years of age), epitheloid sarcoma, and Kaposi sarcoma [28].

Giant cell tumor of the tendon sheath

A giant cell tumor of the tendon sheath is the most common true neoplasm on the hand. They occur most frequently between the ages of 30–50 years [29]. They represent the extra-articular extension of pigmented villonodular synovitis. They develop over a long period of time and they grow outward due to the limited space in the synovial cavity of the tendon sheath. The characteristic MR pattern is intermediate signal on T1 and hypointensity on T2, especially on gradient echo, due to hemosiderin-laden histocytes found in the tumor, and to regions of collagen bands (Fig. 15) [2, 3, 15, 21]. These tumors usually show mild or strong enhancement after IV gadolinium administration, which is more conspicuous on T1 and fat suppression (Fig. 15). Non-enhancement after IV gadolinium administration is an uncommon finding (1 of 8 in our series; Fig. 16). Cortical bone erosion is reported in 10–50% of cases [29]. On US these

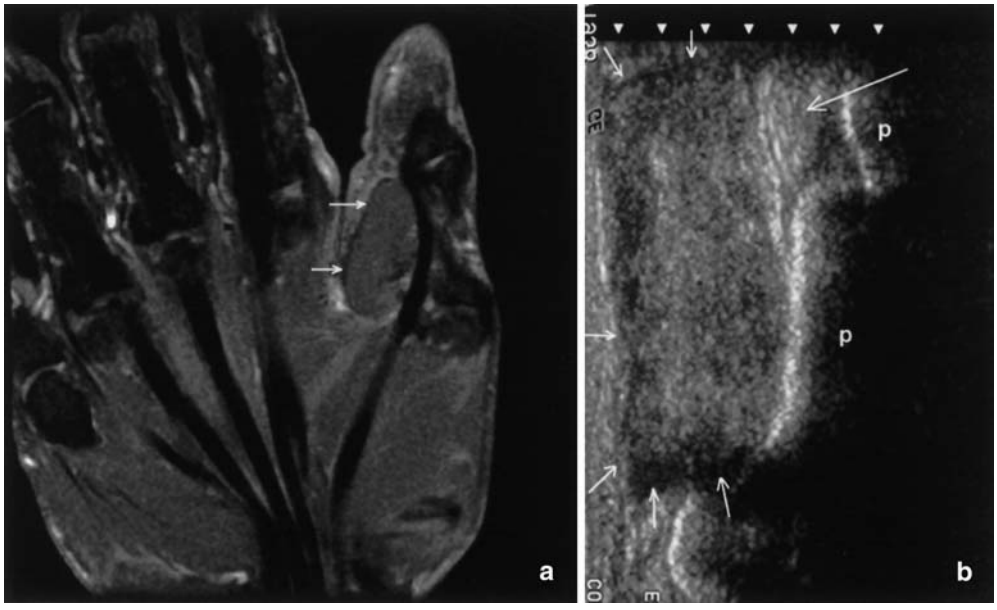

Fig. 16a, b Giant cell tumor of tendon sheath. **a** Coronal contrast-enhanced T1-weighted fat-suppressed SE image (TR/TE/slice thickness: 460ms/13 ms/3 mm). **b** Ultrasound image. This homogeneous tumor (*small arrows*) did not enhance after gadolinium administration. It is exophytically attached to the flexor tendon sheath. *Long arrow* flexor tendon; *p* phalanx

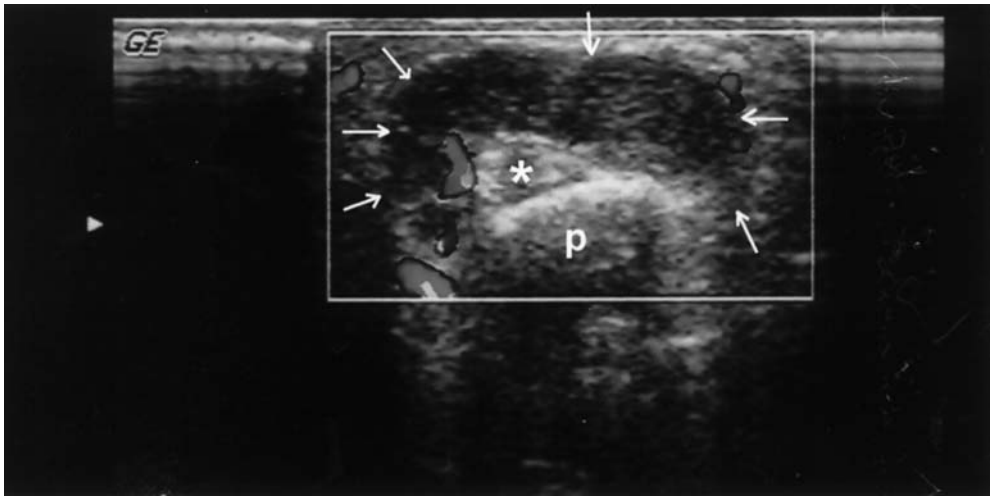

Fig. 17 Homogeneous giant cell tumor (*small arrows*) in axial echo Doppler which displaces the palmar neurovascular bundle without invasion. Ultrasound was enough to make the diagnosis. *Asterisk* tendon; *p* phalanx

tumors usually are homogeneous and hypoechoic lesions with regular or lobulated contours [1, 4, 10]. They do not show evident echo Doppler flow. Although the US pattern is not specific, these findings, plus the intimate relation of the lesion with the tendon sheath, as well as its clinical presentation, may strongly suggest the diagnosis (Fig. 17). The differential diagnosis may be done with those cases of highly hypertrophic atypical tenosynovitis and fibroma of the tendon sheath.

Fibroma of the tendon sheath

Fibroma of the tendon sheath was characterized in 1979 by Chung and Enzinger in a series of 138 cases [30]. It is a rare benign tumor that is more frequent in males, composed of fibroblasts in a dense fibrous stroma. They are usually firm, well-circumscribed masses attached to the tendon sheath, more common in the hands. Rare cases have been reported in the literature arising from synovial joints [31]. To the best of our knowledge, the MR appearance of this tumor has previously been reported in only five cases [31, 32, 33, 34, 35]. It has been demonstrated that these tumors usually show low signal on both T1- and T2-weighted images, and variable enhancement after gadolinium on MR; thus, the differential diagnosis includes desmoid tumor, nodular fascitis, fibrous histiocytoma and giant cell tendon sheath tumor [31, 32, 33]. However, upon revising the published cases, we have noticed that the MR appearance is very variable, proba-

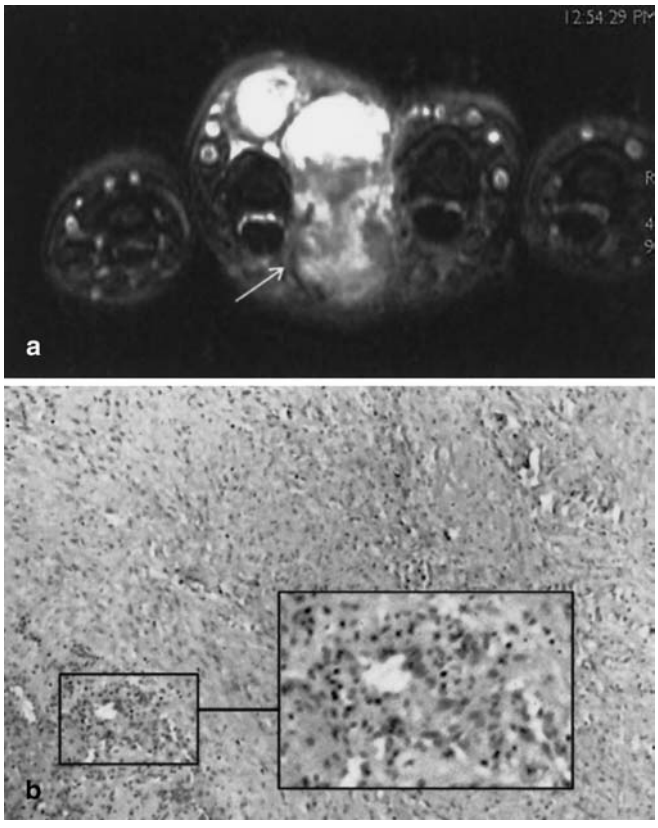

Fig. 18a, b Fibroma of tendon sheath. **a** Axial T2-weighted fat-suppressed FSE image (TR/TE/slice thickness: 4900 ms/85 ms/3 mm). Large, lobulated mass in third interdigital space which surrounds flexor and extensor tendon sheaths. There is invasion of palmar neurovascular bundle of fourth finger (*arrow*). It is a heterogeneous mass with a very high signal on T2. **b** Proliferation of collagenous tissue with multinodular appearance

bly according to their variable vascularization and fibrous content. They may appear, as in our case, hyperintense on gradient echo [33] and hyperintense on T2 (Fig. 18) [34], which helps to distinguish this lesion from the giant cell tumor of the tendon sheath (hypointense on T2), which is its main differential diagnosis, because of its frequency.

Neurofibroma

Solitary neurofibroma is a tumor rising from the nerve sheath, composed of Schwann cells and fibroblasts with neural axons traversing the mass. Typically, it is a benign, non-encapsulated well-circumscribed and slowly growing fusiform tumor that develops between the ages of 20 and 30 years [36]. Neurogenic tumors usually show areas with a higher signal on T1-weighted images and a lower signal on T2-weighted images than other soft tissue masses [37]. They may have a central zone of dense fibers and highly cellular component, and a peripheral zone with less fibers and cellular component but with an abundant non-fibrillary stromal component such as myxoid material. This pattern explains the so-called target appearance in imaging studies and it is an indication of its benign character (Fig. 19) [36]. It is often difficult to distinguish neurofibroma from schwannoma because the imaging findings may be similar in these lesions; however, schwannoma is usually more heterogeneous because of the presence of cysts, necrosis, and hemorrhage, and it is a rounder and more excentric tumor [36, 37].

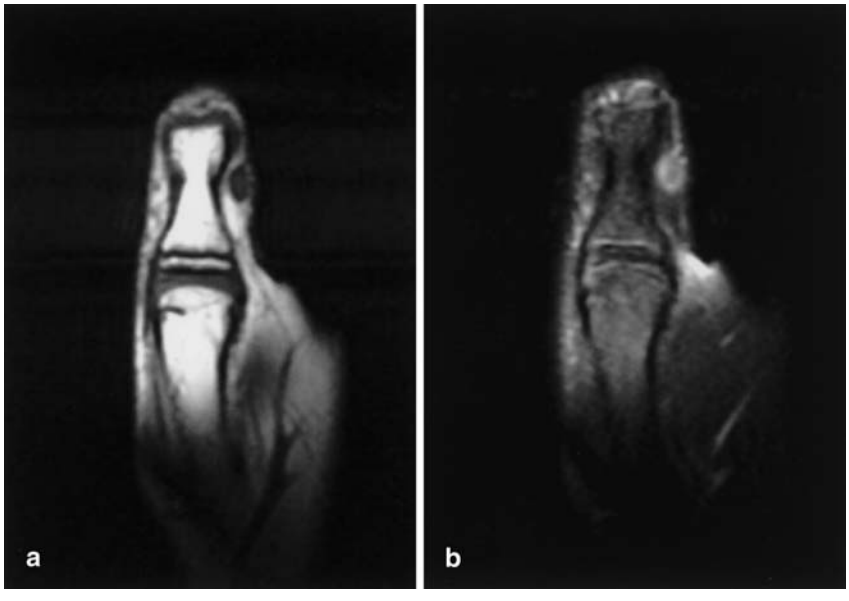

Fig. 19a, b Neurofibroma. **a** Coronal T1-weighted SE image (TR/TE/slice thickness: 440 ms/14 ms/2 mm). **b** Coronal fat-suppressed FSE PD image (TR/TE/slice thickness: 3000 ms/57 ms/2 mm). Small fusiform tumor in cubital side of the first finger with a "target appearance" on T2WI: hyperintense peripheral zone due to non-fibrillary stromal component

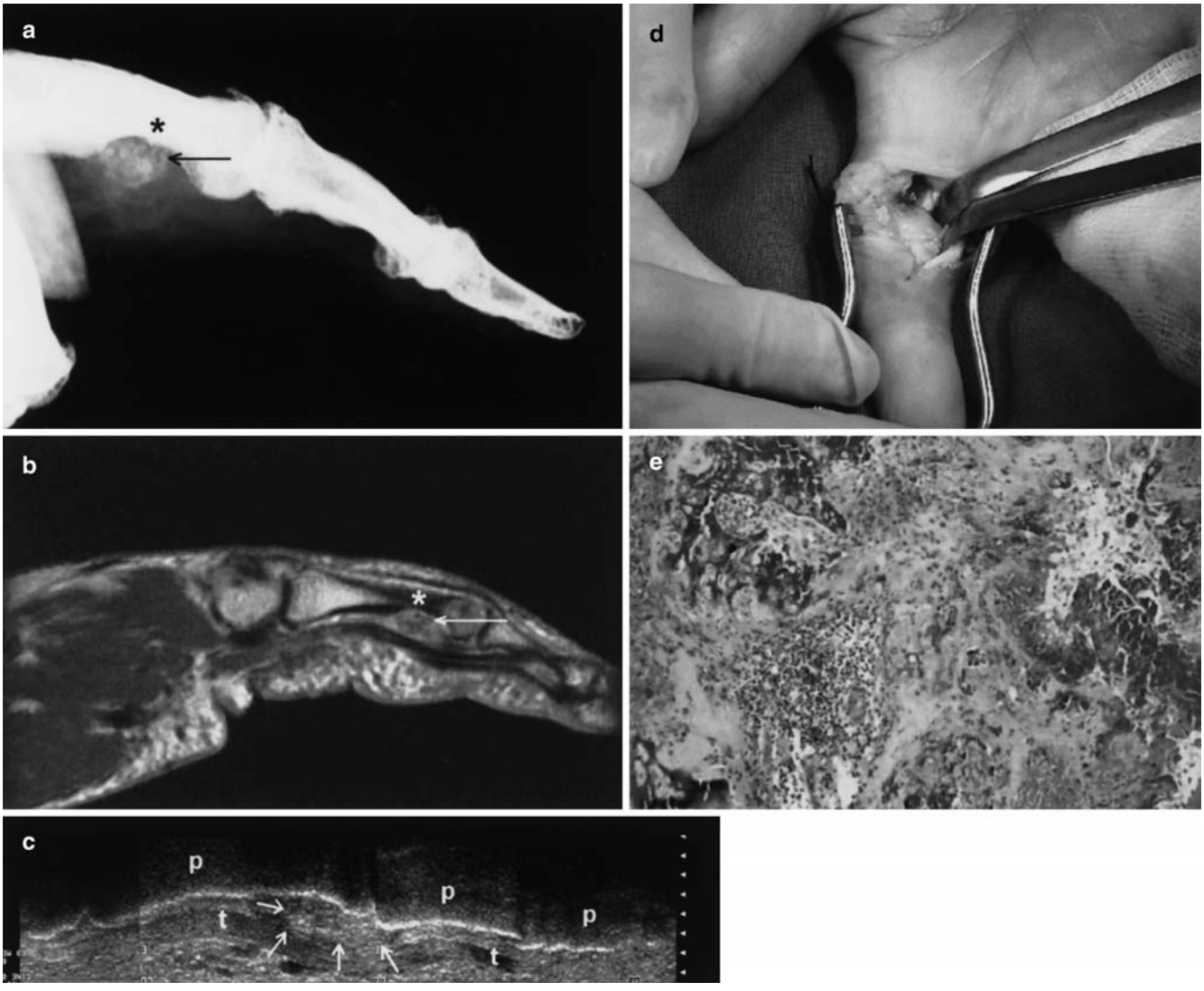

Fig. 20a–e Extraskeletal chondroma. **a** Low-kilovoltage plain film. **b** Ultrasound image. **c** Sagittal gadolinium-enhanced T1-weighted SE image (TR/TE/slice thickness: 40 ms/14 ms/2 mm). Well-defined ovoid nodule (*small arrows*) between the flexor tendon (*arrow* in **a**) and the phalanx, with osseous remodeling secondary to the long-standing mass (*asterisk*). The characteristic chondral annular calcifications are conspicuous in the MR enhanced image (*arrow* in **b**). **d** Intraoperative photograph. **e** Low-power photomicrograph with areas of hyaline cartilage formation and calcifications unattached to bone. It shows chondroblastic and granuloma-like elements. *p* phalanx

Extraskeletal chondroma

Extraskeletal or soft tissue chondroma is an unusual lesion that consists of a well-defined nodule of cartilage that is unattached to bone. These tumors may be seen at any age, although they are most common between the ages of 10–70 years; most of them are located in the extremities, especially in the hands [38, 39, 40]. They present clinically as a slow-growing mass that may cause pain or tenderness. They are small (usually <3 cm in size), firm, and often mobile tumors on palpation [40]. Calcification is seen in 33–70% of the reported cases [38, 39, 40], sometimes with a characteristic ring-like cartilage appearance. Extrinsic bone erosion may be seen (Fig. 20). There is scant literature on the US and MR appearance of soft tissue chondroma. The case of our series presented characteristic annular calcifications inside a mass isointense relative to skeletal muscle on T1WI and hyperintense on T2WI, and gadolinium enhancement (Fig. 20). The histopathologic appearance is variable, ranging from an immature pattern resembling osseous chondroblastoma to a mature profile similar to enchondroma. A granuloma-like reaction may be seen within the stroma [40, 41, 42]. The differential diagnosis should include benign calcified intra-articular lesions (synovial chondromatosis, solitary intra-articular chondroma, and periostal chondroma) or

malignant lesions (extraskeletal myxoid chondrosarcoma) [38, 39, 40].

Conclusion

A highly accurate finger lesion diagnosis is obtained with MR lesion characterization in most of the cases (more than 80% in our series), taking into account the patient's clinical history and plain films. Ultrasound is a less time-consuming and less expensive technique that constitutes, in trained hands, an excellent alternative in many cases. Sometimes US and MR are complementary techniques. To obtain a correct presurgical diagnosis it is of utmost importance to possess an in-depth knowledge of finger radiological anatomy in detail, as well as the appearance of the different pathologic entities on both US and MR.

Acknowledgements We thank J.C. Albillos, T. Hernandez, and J.A. Martinez for their computer assistance in producing the images. We especially thank T. Fontanilla and M.F. and A. Horrocks for reading the manuscript.

References

1. Fornage BD, Rifkin MD (1988) Ultrasound examination of the hand and foot. Radiol Clin North Am 26:109–129
2. Peth WC, Truong NP, Totty WG, Gilula LA (1995) Pictorial review: magnetic resonance imaging of benign soft tissue mases of the hand and wrist. Clin Radiol 50:519–525
3. Capelastegui A, Astigarraga E, Fernandez-Canton G, Saralegui I, Larena JA, Merino A (1999) Masses and pseudomasses of the hand and wrist: MR findings in 134 cases. Skeletal Radiol 28:498–507
4. Creteur V, Peetrons P (2000) Echographie du poignet et de la main. J Radiol 81:346–352
5. Savnik A, Malmskov H, Thomsen HS, Bretlau T, Graff LB, Nielsen H, Danneskiold-Samsoe B, Boesen J, Bliddal H (2001) MRI of the arthritic small joints: comparison of extremity MRI (0.2 T) vs high-field MRI (1.5 T). Eur Radiol 11:1030–1038
6. Backhaus M, Kamradt T, Sandrock D, Loreck D, Fritz J, Wolf KJ, Raber H, Hamm B, Burmester GR, Bollow M (1999) Arthritis of the finger joints: a comprehensive approach comparing conventional radiography, scintigraphy, ultrasound, and contrast-enhanced magnetic resonance imaging. Arthritis Rheum 42:1232–1245
7. Hergan K, Mittler C, Oser W (1997) Pitfalls in sonography of the Game keeper's thumb. Eur Radiol 7:65–69
8. Van-Sint-Jan S, Rooze M, Van-Audekerke J, Vico L (1996) The insertion of the extensor digitorum tendon on the proximal phalanx. J Hand Surg [Am] 21:69–76
9. Serafini G, Derchi LE, Quadri P, Martinoli C, Orio O, Cavallo A, Gandolfo N (1996) High resolution sonography of the flexor tendons in trigger fingers. J Ultrasound Med 15:213–219
10. Martinoli C, Bianchi S, Derchi LE (1999) Tendon and nerve sonography. Radiol Clin North Am 37:691–711
11. Doyle JR (1989) Anatomy of the flexor tendon sheath and pulley system: a current review. J Hand Surg [Am] 14:349–351
12. Cresswell TR, Allott C, Auchincloss JM (1998) Colour Doppler ultrasound in the diagnosis, management and follow-up of a digital flexor pulley injury. J Hand Surg [Br] 23:655–657
13. Lewis AR, Nolan MJ, Hodgson RJ, Benjamin M, Ralphs JR, Archer, CW, Tyler JA, Hall LD (1996) High resolution magnetic resonance imaging of the proximal interphalangeal joints. Correlation with histology and production of a three-dimensional data set. J Hand Surg [Br] 21:488–495
14. Boudghene FP, Gouny P, Tassart M, Callard P, Le Breton C, Vayssairat M (1998) Subungual glomus tumor: combined use of MRI and three-dimensional contrast MR angigraphy. J Magn Reson Imaging 8:1326–1328
15. Van Goethem JWM, Shahabpour M (1997) Synovial tumors. In: De Schepper AM (ed) Imaging of soft tissue tumors. Springer, Berlin Heidelberg New York, pp 255–269
16. Drape JL, Idy-Peretti I, Goettmann S, Salon A, Abimelec P, Guerin-Surville H, Bittoun J (1996) MR imaging of digital mucoid cysts. Radiology 200:531–536
17. De Flaviis L, Musso MG (1995) Hand and wrist. Clin Diagn Ultrasound 30:151–178
18. Howden MD (1994) Foreign bodies within finger tendon sheaths demonstrated by ultrasound: two cases. Clin Radiol 49:419–420
19. Jevtic V, Watt I, Rozman B, Kos-Golja M, Praprotnik S, Logar D, Presetnik M, Demsar Fjarh O, Campion G, Musikic P (1997) Contrast enhanced Gd-DTPA magnetic resonance imaging in the evaluation of rheumatoid arthritis during a clinical trial with DMARDs. A prospective two-year follow-up study on hand joints in 31 patients. Clin Exp Rheumatol 15:151–156
20. Van-Vught RM, Van-Dalen A, Bijlsma JW (1998) The current role of high-resolution ultrasonography of the hand and wrist in rheumatic diseases. Clin Exp Rheumatol 16:454–458
21. Ma LD, McCarthy EF, Bluemke DA, Frassica FJ (1998) Differentiation of benign from malignant musculoskeletal lesions using MR imaging: pitfalls in MR evaluation of lesions with a cystic appearance. Am J Roentgenol 170:1251–1258
22. Binkovitz LA, Berquist TH, McLeod RA (1990) Masses of the hand and wrist: detection and characterization with MR imaging. Am J Roentgenol 154:323–326
23. Marques MC, Garcia H (1997) Lipomatous tumors. In: De Schepper AM (ed) Imaging of soft tissue tumors. Springer, Berlin Heidelberg New York, pp 191–207
24. Enzinger FW, Weiss SW (1995) Benign tumors and tumorlike lesions of blood vessels. In: Enzinger FM, Weiss SW (eds) Soft tissue tumors, 3rd edn. Mosby, St. Louis, pp 579–626
25. Ramon F (1997) Tumors and tumorlike lesions of blood vessels. In: De Schepper AM (ed) Imaging of soft tissue tumors. Springer, Berlin Heidelberg New York, pp 209–227

26. Theumann NH, Bittoun J, Goettmann S, Le Viet D, Chevrot A, Drapé JL (2001) Hemangiomas of the fingers: MR imaging evaluation. Radiology 218:841–847
27. Lawson GM, Salter DM, Hooper G (1995) Angioleiomyomas of the hand. A report of 14 cases. J Hand Surg [Br] 20:479–483
28. Kransdorf MJ (1995) Malignant soft-tissue tumors in a large referral population: distribution of diagnoses by age, sex and location. Am J Roentgenol 164:129–134
29. Jones FE, Soule EH, Coventry MB (1969) Fibrous histiocytoma of synovium (giant cell tumor of tendon sheath, pigmented nodular synovitis). A study of 118 cases. J Bone Joint Surg [Am] 51:76–86
30. Chung EB, Enzinger FM (1979) Fibroma of tendon sheath. Cancer 44:1945–1954
31. Misawa A, Okada K, Hirano Y, Sageshima M (1999) Fibroma of tendon sheath arising from the radio-ulnar joint. Pathol Int 49:1089–1092
32. De Schepper AM, Vandevenne JE (1997) Tumors of fibrous tissue. In: De Schepper AM (ed) Imaging of soft tissue tumors. Springer, Berlin Heidelberg New York, pp 147–172
33. Bertolotto M, Rosenberg I, Parodi RC, Perrone R, Gentile S, Rollandi GA, Succi S (1996) Case report: fibroma of tendon sheath in the distal forearm with associated median nerve neuropathy: US, CT and MR appearances. Clin Radiol 51:370–372
34. Hur J, Damron TA, Vermont AI, Mathur SC (1999) Fibroma of tendon sheath of the infrapatellar fat pad. Skeletal Radiol 28:407–410
35. Pinar H, Ozkan M, Ozaksoy D, Pabuccuoglu, Akseki D, Karaoglan O (1995) Intraarticular fibroma of the tendon sheath of the knee. Arthroscopy 11:608–611
36. Parizel PM, Simoens WA, Matos C, Verstraete KL (1977) Tumors of peripheral nerves. In: De Schepper AM (ed) Imaging of soft tissue tumors. Springer, Berlin Heidelberg New York, pp 271–298
37. Simoens WA, Wuyts FL, De Beuckeleer LH, Vandevenne JE, Bloem JL, De Schepper AM (2001) MR features of peripheral nerve sheath tumors: Can a calculated index compete with radiologist's experience? Eur Radiol 11:250–257
38. Kransdorf MJ, Meis JM (1993) Extraskeletal osseous and cartilaginous tumors of the extremities. Radiographics 13:853–884
39. Zlatkin MB, Lander PH, Begin LR, Hadjipavlou A (1985) Soft tissue chondromas. Am J Roentgenol 144:1263–1267
40. Chung EB, Enzinger FM (1978) Chondroma of soft parts. Cancer 41:1414–1424
41. Isayama T, Iwasaki H, Kikuchi M (1991) Chondroblastomalike extraskeletal chondroma. Clin Orthop 268:214–217
42. Yamada T, Irisa T, Nakano S, Tokunaga O (1995) Extraskeletal chondroma with chondroblastic and granuloma like elements. Clin Orthop 315:257–261